J. Mater. Environ. Sci. 6 (10) (2015) 2906-2916
ISSN : 2028-2508
CODEN: JMESCN

The role of new phosphonate derivatives on the corrosion inhibition of mild steel in 1M H_2SO_4 media

Y. Kharbach[1], A. Haoudi[1], M.K. Skalli[1], Y. Kandri Rodi[2], A. Aouniti[3], B. Hammouti[3], O. Senhaji[4], A. Zarrouk[3]

[1]*Laboratory of.Applied Chemistry, U.S.M.B.A., Faculty of Science and Technology of Fes, Morocco.*
[2]*Laboratory of.Applied Organic Chemistry, U.S.M.B.A., Faculty of Science and Technology of Fes, Morocco.*
[3] *LCAE-URAC18, Faculty of Science, Mohammed first University, Po Box 717, 60000 Oujda, Morocco.*
[4]*Laboratory of Applied Physical Chemistry. UMI., Faculty of Sciences and Technology of Errachidia, Morocco.*

Received 07 Nov 2014, Revised 31 Oct 2015, Accepted 01 Nov 2015
** Corresponding author. E-mail address: ossenhaji@yahoo.fr*

Abstract
The inhibition performances of sodium methyldodecylphosphonate (Pho1) and sodium methyl (11-methacryloyloxyundecyl) phosphonate (Pho2) on mild steel corrosion insulfuric acid solution were studied using the electrochemical impedance spectroscopy (EIS) and Tafel polarization techniques. The experimental results suggest that those compounds are effective corrosion inhibitors and the inhibition efficiency increases with the increase ininhibitors concentrations. Polarization measurements proved that the inhibitors behave as mixed-type. EIS diagram appears a large capacitive loop at high frequencies (HF) followed by a small inductive loop at low frequencies (LF) for Pho2, and the addition of this inhibitor increases the impedance of electrode. The adsorption of each inhibitor on steel surface obeys Langmuir adsorption isotherm. The thermodynamic and kinetic parameters were calculated and discussed. Values of inhibition efficiency calculated from weight loss, Tafel polarization curves, and EIS are in good agreement.

*Keywords***:** Mild steel, H_2SO_4, Corrosion inhibition, EIS, Polarization, Weight loss.

1. Introduction

Acid solutions are widely used in industry. The corrosion of steel in acidic solution receives considerable concern. Sulfuric acid is one of the most aggressive acids for iron and its alloys and is often used during cleaning, pickling, descaling, acidizing, we use corrosion inhibitors to reduce the corrosion rates of metallic materials in acidic media [1-2].

The use of corrosion inhibitors is one of the most practical methods for protection of steel against corrosion in acidic solutions. Most of well known acid corrosion inhibitors are organic compounds containing nitrogen, sulfur or oxygen atoms [3-8]. Those organic inhibitors molecules apply their inhibition action via the adsorption of the inhibitor molecules onto the metal/solution interface [9-12]. The adsorption process is affected by the chemical structures of the inhibitors, the nature and charged surface of the metal and the distribution of charge over the whole inhibitor molecule.

The phosphonate derivatives have been successfully used as corrosion inhibitors in many practical applications, and they are effective corrosion inhibitors for aluminum, copper and steel in hydrochloric, nitric and sulfuric acid solutions [13-17]. The encouraging results obtained by these compounds have incited us to test their effect on the corrosion behaviour of mild steel insulfuric acidic media (1M H_2SO_4).

In this article, we are interesting to investigate the corrosion inhibition of mild steel in sulfuric acid by two already synthesized phospohonate derivatives [18,19] (scheme 1) namely sodium methyldodecylphosphonate (Pho1) and sodium methyl (11-methacryloyloxyundecyl) phosphonate (Pho2). The chemical structures of those compounds are given in scheme 1. The corrosion inhibitive activity of those organic compounds was examined successively via

weight loss, potentiodynamic polarization curves, electrochemical impedancespectroscopy (EIS). The kinetic and adsorption parameters of corrosion inhibition process are also evaluated.

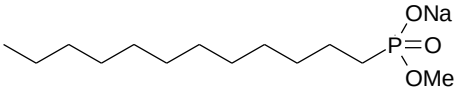 Sodium methyldodecylphosphonate	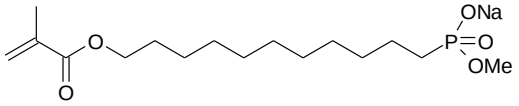 Sodium methyl (11-methacryloyloxyundecyl)phosphonate
Pho1	Pho2

Scheme 1: Chemical formulas of Pho1 and Pho2.

2. Experimental section

2.1. Materials

The steel used in this study is a mild steel with a chemical composition (in wt%) of 0.09%P, 0.01 % Al, 0.38 % Si, 0.05 % Mn, 0.21 % C, 0.05 % S and the remainder iron (Fe). The steel samples were pre-treated prior to the experiments by grinding with amery paper sic (220, 400, 800, 1000 and 1200); rinsed with distilled water, degreased in acetone, washed again with bidistilled water and then dried at room temperature before use.

2.2. Solutions

The aggressive solutions of 1M H_2SO_4 were prepared by dilution of analytical grade 97% H_2SO_4 with distilled water. The concentration range of sodium methyldodecylphosphonate (Pho1) and sodium methyl (11-methacryloyloxyundecyl) phosphonate (Pho2) used was 10^{-6}M to 10^{-3}M.

2.3. Gravimetric study

Gravimetric experiments were performed according to the standard methods, the mild steel sheets of 1.5 cm × 1.5 cm × 0.03 cm were abraded with a series of emery papers sic (220, 400, 800, 1000 and 1200) and then washed with distilled water and acetone. After weighing accurately, the specimens were immersed in a 50 mL beaker containing 100 mL of 1 M H_2SO_4 solution with and without addition of different concentrations inhibitor. All the aggressive acid solutions were open to air. After 6 h of acid immersion, the specimens were taken out, washed, dried, and weighed accurately. In order to get good reproducibility, all measurements were performed few times and average values were reported to obtain good reproducibility. The inhibition efficiency (η_{WL}%) and surface coverage (θ) were calculated as follows:

$$C_R = \frac{W_b - W_a}{At} \quad (1)$$

$$\eta_{WL}(\%) = \left(1 - \frac{w_i}{w_0}\right) \times 100 \quad (2)$$

$$\theta = \left(1 - \frac{w_i}{w_0}\right) \quad (3)$$

where W_b and W_a are the specimen weight before and after immersion in the tested solution, w_0 and w_i are the values of corrosion weight losses of mild steel in uninhibited and inhibited solutions, respectively, A the total area of the mild steel specimen (cm^2) and t is the exposure time (h).

2.4. Electrochemical measurements

The electrochemical measurements were carried out using Volta lab (Tacussel- Radiometer PGZ 100) potentiostate and controlled by Tacussel corrosion analysis software model (Voltamaster 4) at under static condition. The corrosion cell used had three electrodes. The reference electrode was a saturated calomel electrode (SCE). A platinum electrode was used as auxiliary electrode of surface area of 1 cm^2. The working electrode was mild steel of the surface 0.04

cm^2. All potentials given in this study were referred to this reference electrode. The working electrode was immersed in test solution for 30 min to a establish steady state open circuit potential (E_{ocp}). After measuring the E_{ocp}, the electrochemical measurements were performed. All electrochemical tests have been performed in aerated solutions at 308 K. The EIS experiments were conducted in the frequency range with high limit of 100 kHz and different low limit 0.1 Hz at open circuit potential, with 10 points per decade, at the rest potential, after 30 min of acid immersion, by applying 10 mV ac voltage peak-to-peak. Nyquist plots were made from these experiments. The best semicircle can be fit through the data points in the Nyquist plot using a non-linear least square fit so as to give the intersections with the *x*-axis.

After ac impedance test, the potentiodynamic polarization measurements of mild steel substrate in inhibited and uninhibited solution were scanned from cathodic to the anodic direction, with a scan rate of 1 mV s^{-1}. The potentiodynamic data were analysed using the polarization VoltaMaster 4 software. The linear Tafel segments of anodic and cathodic curves were extrapolated to corrosion potential to obtain corrosion current densities (I_{corr}).

3. Results and discussion

3.1. Polarization Measurements

Potentiodynamic polarization data of various concentrations of Pho1 and Pho2 are shown as the Tafel plots steel in 1 M H_2SO_4 in Figures 1 and 2. The corrosion kinetic parameters such as corrosion potential (E_{corr}), corrosion current density (I_{corr}), cathodic Tafel slopes (β_c) were derived from these curves and are given in Table1.

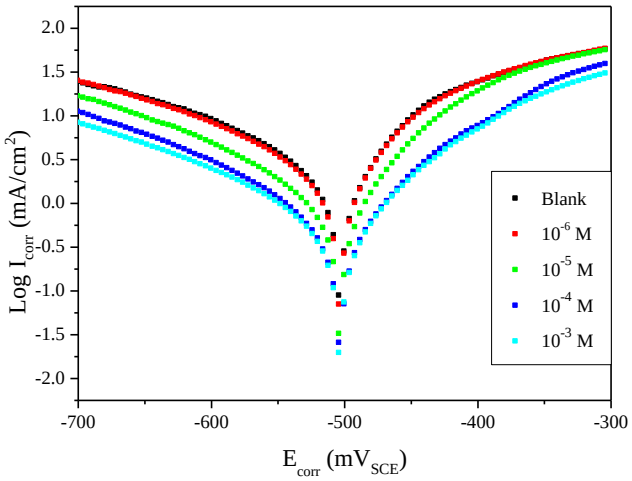

Figure 1: Polarization curves of steel in 1M H_2SO_4 containing various concentrations of Pho1.

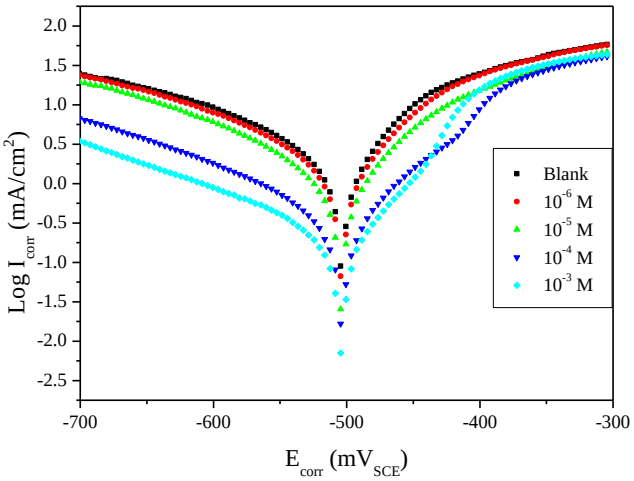

Figure 2: Polarization curves of steel in 1M H_2SO_4 containing various concentrations of Pho2.

The values of inhibition efficiency (E_I%) were calculated using the following equation:

$$E_I\% = \frac{I_{corr} - I_{corr\ (inh)}}{I_{corr}} \times 100 \quad (1)$$

Where I_{corr} and $I_{corr(inh)}$ are the values of corrosion current densities of steel without and with the additive, respectively, which were determined by extrapolation of the cathodic Tafel lines to the corrosion potential E_{corr}.

Table 1. Electrochemical data of steel at various concentrations of Pho1 and Pho2 in 1M H_2SO_4 and corresponding inhibition efficiencies.

	Conc (M)	$-E_{corr}$ (mV/SCE)	$-\beta_c$ (mV/dec)	I_{corr} (µA/cm²)	E_I (%)
Blank	1	503	144	1990	—
Pho1	10^{-6}	505	138	1870	6.0
	10^{-5}	501	120	1060	46.7
	10^{-4}	504	203	928	53.3
	10^{-3}	504	122	519	73.9
Pho2	10^{-6}	498	184	1880	5.5
	10^{-5}	500	133	1560	21.6
	10^{-4}	493	168	490	75.3
	10^{-3}	478	172	240	87.9

The data in Table 1 indicate that in both cases I_{corr} values gradually decreased with the increase of the inhibitor concentration with respect to the blank. Inhibition efficiency (E_I) at 10^{-3} M reaches up to a maximum of 87.9% for Pho2; and 73.9% for Pho1, which again confirms that both inhibitors are good inhibitors for steel in 1 M H_2SO_4, and E_I follows the order: Pho2 > Pho1. According to the literature [20], it has been reported that (i) if the shift in E_{corr} is < 85 mV the inhibitor can be claimed as mixed type and (ii) if the shift in E_{corr} is > 85 mV, with repect to E_{corr}, the inhibitor behave as either cathodic or anodic. In this investigation, the shift in E_{corr} is less than 25 mV for Pho2 and is even less for Pho1, suggesting that both Pho2 and Pho1 act as mixed type of inhibitors [21].

3.2. Electrochemical Impedance Spectroscopy (EIS)

EIS was carried out on a newly polished steel surface in acidic solution in the absence and presence of Pho2 at open circuit potential at 308 K after 30 min of immersion. Nyquist plots of steel in 1M H_2SO_4 in the presence and absence of additive are given in Figure 3. These curves have obtained after 30 min of immersion in the corresponding solution. Impedance parameters derived from the Nyquist plots are given in Table 2. The charge transfer resistance, R_t values are calculated from the difference in impedance at lower and higher frequencies. To obtain the double layer capacitance (C_{dl}), the frequency at which the imaginary component of the impedance is maximum ($-Z_{max}$) is found and C_{dl} values are obtained from the equation:

$$f(-Z_{max}) = \frac{1}{2\pi C_{dl} R_t} \quad (4)$$

Fig. 3 represent the Nyquist diagrams for mild steel in 1 M H_2SO_4 in the presence of Pho2, respectively. Clearly, the impedance spectra exhibit a large capacitive loop at high frequencies followed by a small inductive loop at low frequency values. In the presence of Pho2, comparing with blank solution, the shape is maintained throughout all tested concentrations, indicating that almost no change in the corrosion mechanism occurs due to the inhibitor addition [22]. The capacitive loop indicates that the corrosion of steel is mainly controlled by a charge transfer process, and usually related to the charge transfer of the corrosion process and double layer behavior. On the other hand, the inductive loop may be attributed to the relaxation process obtained by adsorption species like $FeSO_4$ [23] or inhibitor species [24] on the electrode surface.

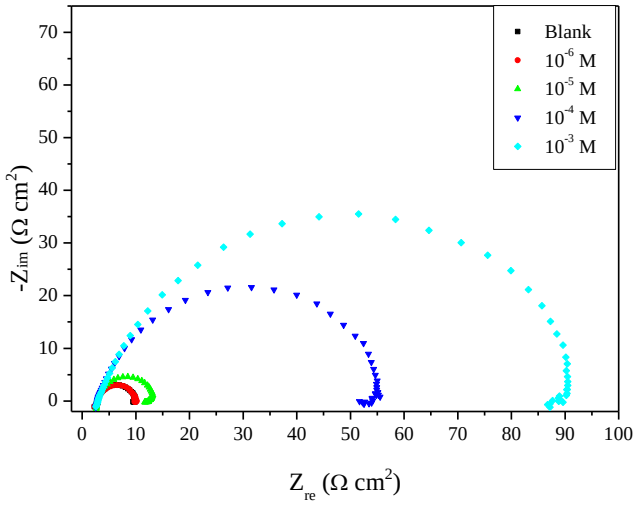

Figure 3: Nyquist diagrams for steel in 1M H_2SO_4 containing different concentrations of Pho2.

The diameter of the capacitive loop in the presence of inhibitor is bigger than that in the absence of inhibitor (blank solution) and increases with the inhibitor concentration. This indicates that the impedance of inhibited substrate increases with the inhibitor concentration. Noticeably, these capacitive loops are not perfect semicircles which can be attributed to the frequency dispersion effect as a result of the roughness and inhomogeneousness of the electrode surface [25].

Table 2: Characteristic parameters evaluated from the impedance diagram for steel in 1M H_2SO_4 at various concentrations of Pho2.

	Conc (M)	R_t (Ω cm^2)	C_{dl} (μF/cm^2)	E (%)
Blank	1	4.99	100.7	--
Pho2	10^{-6}	7.15	70.27	30
	10^{-5}	9.67	51.96	48
	10^{-4}	51.48	38.91	90
	10^{-3}	83.41	30.16	94

Data in Table 2 shows that additional Pho2 inhibits the corrosion of mild steel in 1M H_2SO_4. The inhibition efficiency is calculated using charge transfer resistance from the equation [26]:

$$E_{R_t}\% = \frac{R_{tcorr(inh)} - R_{tcorr}}{R_{tcorr(inh)}} \quad (5)$$

Where R_{tcorr} and $R_{tcorr(inh)}$ are the charge transfer resistance values in absence and presence of inhibition for steel in 1M H_2SO_4, respectively.

By increasing the inhibitor concentration the R_t values increase but C_{dl} values decrease. According to Helmoltz model, the double layer capacitance C_{dl} is given by:

$$C_{dl} = \frac{\varepsilon_0 \varepsilon}{\delta} S \quad (6)$$

Where δ is the thickness of the deposit, S is the surface of the electrode, ε_0 is the permittivity of the air, and ε is the medium dielectric constant.

As can be seen from this Table 2 and figure 4 the decrease in C_{dl}, which can result from a decrease in local dielectric constant and/or an increase in the thickness of the electric double layer [27,28], suggested that Pho2 molecules

function by adsorption at the metal/solution interface. Thus, the decrease in C_{dl} values and the increase in R_t values and consequently of inhibition efficiency may be due to the gradual replacement of water molecules by the adsorption of the Pho molecules on the metal surface, decreasing the extent of dissolution reaction [29].

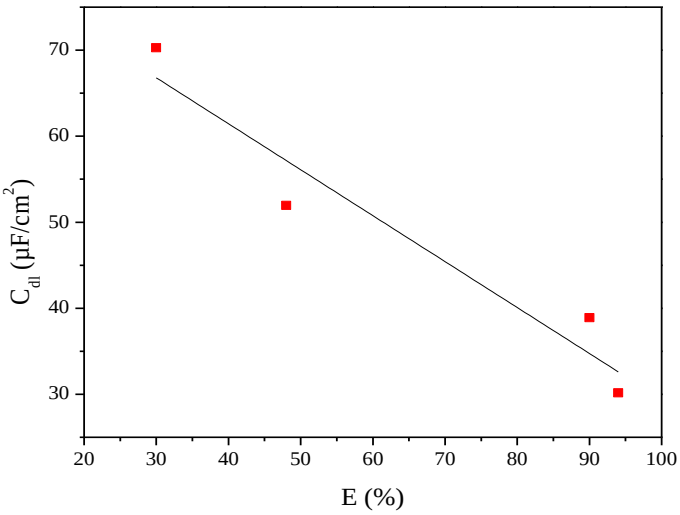

Figure 4: Evolution of C_{dl} with the inhibition efficiency of Pho2.

3.3. Weight Loss Tests

3.3.1. Effect of concentration

Table 3, collects the corrosion rates and the inhibition efficiencies evaluated from weight loss measurements for different inhibitor concentrations in 1M H_2SO_4. The corrosion rate reduces after addition of the selected two compounds, and decreases with the inhibitor concentration. This behaviour is due to the fact that the adsorption coverage increases with the increase of inhibitor concentration, which shields the mild steel surface efficiently from the medium. In the absence of inhibitor, the corrosion rate is as high as 10.74 mg cm^{-2} h^{-1}. While in the presence of 10^{-3} M inhibitor, the corrosion rate values are reduced to 5.427 and 1.596 mg cm^{-2} h^{-1} for Pho1 and Pho2, respectively. At any given inhibitor concentration, the corrosion rate follows the order: C_R (Pho2) < C_R (Pho1), which indicates that Pho2 exhibits the best inhibitive performance among two compounds.

Table 3: Gravimetric results of steel in acid without and with addition of Pho1 and Pho2 at 6h at 308 K.

Inhibitor	Conc (M)	C_R (mg/cm^2 h)	η_{WL} (%)	θ
Blank	1	10.74	--	--
Pho1	1×10^{-6}	9.969	7.2	0.072
	1×10^{-5}	9.812	8.6	0.086
	5×10^{-5}	9.692	9.6	0.096
	1×10^{-4}	7.563	29.6	0.296
	5×10^{-4}	5.437	49.4	0.494
	1×10^{-3}	5.427	49.5	0.495
Pho2	1×10^{-6}	9.741	9.3	0.093
	1×10^{-5}	9.671	10.0	0.100
	5×10^{-5}	8.42	21.6	0.216
	1×10^{-4}	7.868	26.7	0.267
	5×10^{-4}	1.978	81.6	0.816
	1×10^{-3}	1.596	85.1	0.851

3.3.2. Effect of temperature and thermodynamic activation parameters

Temperature has a great effect on the corrosion phenomenon. Generally the corrosion rate increases with the rise of the temperature. For this purpose, we made weight loss experiments in the range of temperature 313-353 K, in the absence and presence of various concentrations of Pho1 and Pho2 after 1h of immersion.The corresponding data are shown in Table 4, it is clear that the inhibition efficiencies decrease with the increase of temperature.

Table 4: Inhibition efficiencies obtained from the corrosion rate 10^{-3} M of phosphonates in 1M H_2SO_4 at different temperatures at 1h.

Temp (K)	Inhibitors	C_R (mg/cm^2 h)	η_{WL} (%)	θ
313	Blank	21.713	—	—
	Pho1	3.511	83.8	0.83
	Pho2	1.106	94.9	0.94
323	Blank	34.358	—	—
	Pho1	8.627	74.8	0.74
	Pho2	4.747	86.1	0.86
333	Blank	47.007	—	—
	Pho1	20.296	56.8	0.56
	Pho2	15.629	66.7	0.66
343	Blank	62.796	—	—
	Pho1	48.644	22.5	0.22
	Pho2	37.290	40.6	0.40
353	Blank	88.494	—	—
	Pho1	80.766	8.7	0.08
	Pho2	66.494	24.8	0.24

Figure 5 shows that the corrosion rate increases as temperature rises, and the values of inhibition efficiency of Pho2 is more than Pho1.The results show that the inhibition efficiencies decrease with increasing temperature, indicating that at higher temperature dissolution of steel predominates over inhibitor adsorption at the surface.

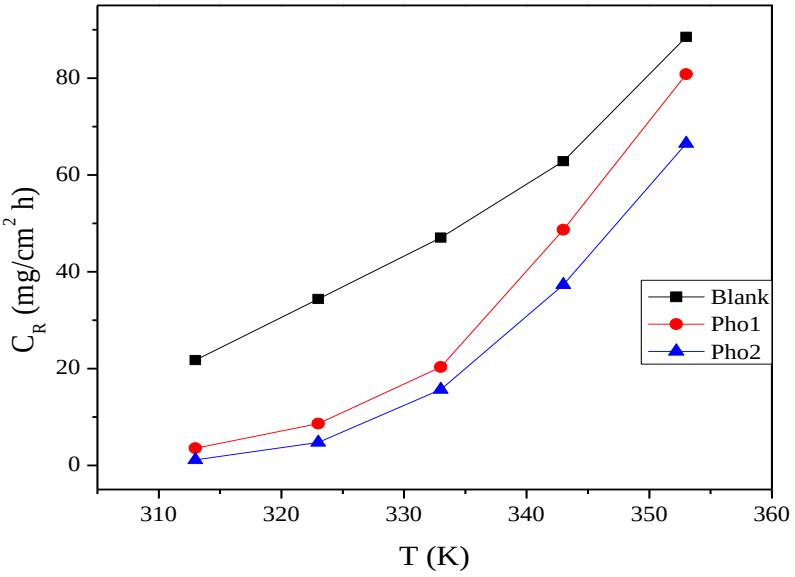

Figure 5: Variation of corrosion rate with temperature of steel at 10^{-3} M of inhibitors.

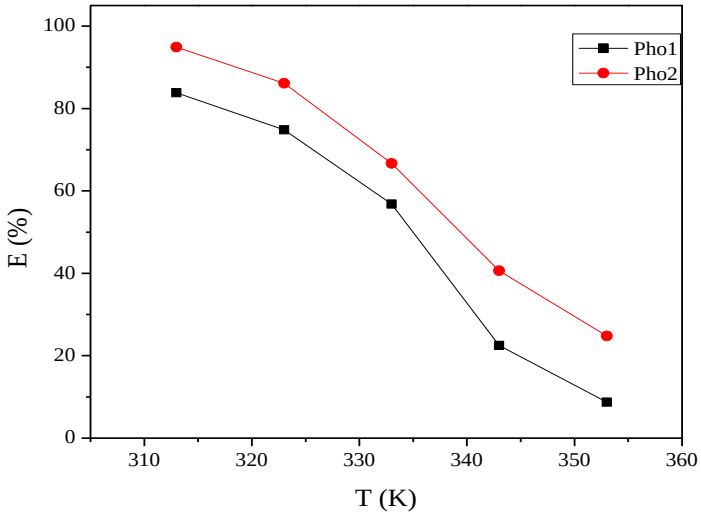

Figure 6: Variation of inhibition efficiency with temperature of steel at 10^{-3} M of inhibitors.

The activation parameters for the corrosion process were calculated from Arrhenius type plot according to the following:

$$C_R = A\exp\left(-\frac{E_a}{RT}\right) \quad (7)$$

Where E_a is the apparent activation corrosion energy, T is the absolute temperature, A is the Arrhenius pre-exponential constant and R is the universal gas constant.

And the alternative formulation of Arrhenius equation is:

$$C_R = \frac{RT}{Nh}\exp\left(\frac{\Delta S_a}{R}\right)\exp\left(-\frac{\Delta H_a}{RT}\right) \quad (8)$$

Where h is Planck's constant, N is Avagadro's number, ΔS_a is the entropy of activation and ΔH_a is the enthalpy of activation.

Arrhenius plots for the corrosion rate of steel are given in (Figure 7). Values of (E_a) for steel in 1 M H_2SO_4 without and with optimum concentrations of Pho1 and Pho2 were calculated by linear regression between Ln (C_R) and 1/T.

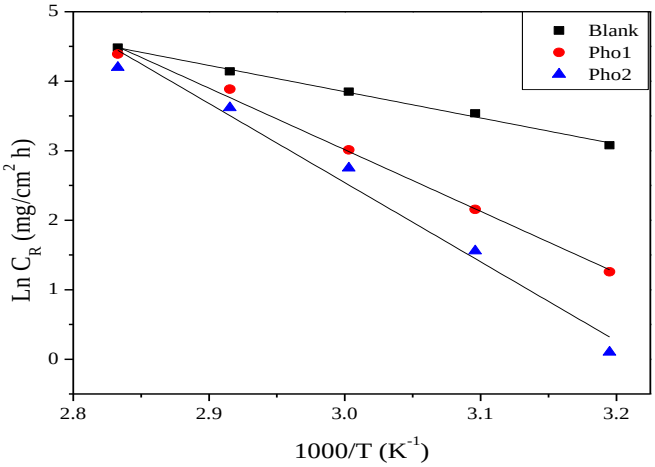

Figure 7: Arrhenius plots of steel for 10^{-3} M of Pho1 and Pho2 in 1M H_2SO_4

Results are shown in (Table 5). All the linear regression coefficients are close to 1. The decrease of inhibition efficiencies with increasing temperature and the increase of E_a in the presence of the inhibitor indicate the physical adsorption mechanism [30].

Figure 8 shows the variation of Ln (C_R/T) function (1/T) as a straight line with a slope of (-H_a / R) and the intersection with the y-axis is [Ln(R/Nh) + (ΔS_a / R)]. From these relationships, values of ΔS_a and ΔH_a can be calculated. The activation parameters (E_a, ΔH_a and ΔS_a) calculated from the slopes of Arrhenius lines in the absence and presence of our inhibitors (Fig.7 and Fig.8) are summarized in Table 5.

Inspection of these data reveals that the ΔH_a values for dissolution reaction of steel in 1M H_2SO_4 in the presence of inhibitors are higher than that of the absence of inhibitors.The positive signs of ΔH_a reflect the endothermic nature of the steel dissolution process suggesting that the dissolution of steel is slow in the presence of inhibitors [31].

Moreover, for all systems, the average value of the difference between E_a and ΔH_a is about 2.8 kJ mol^{-1} which approximately around the average value of RT (2.68 kJ mol^{-1})

$$E_a - \Delta H_a = RT \quad (9)$$

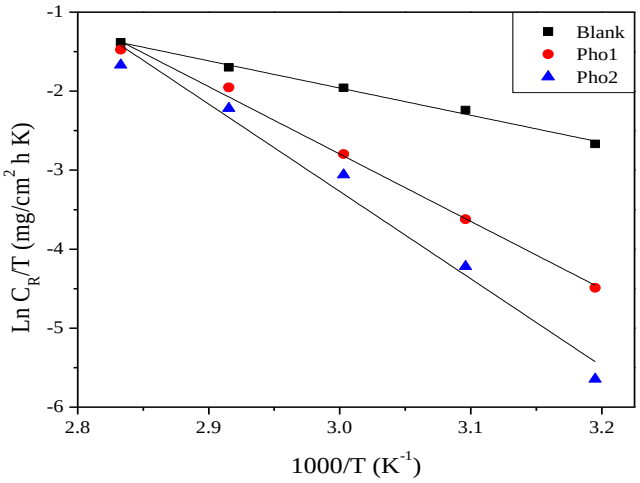

Figure 8: Plots of Ln (C_R/T) against T^{-1} for 10^{-3} of Pho1 and Pho2 in 1M H_2SO_4

Table 5: Values of activation parameters (E_a, ΔH_a, ΔS_a) for steel in 1M H_2SO_4in the absence and presence of Pho1 and Pho2

	Linear regression coefficient (r)	E_a (kJ/mol)	ΔH_a (kJ/mol)	ΔS_a (J/mol K)
Blank	0.996	31.3	28.6	-127.7
Pho1	0.995	73.6	70.8	-8.03
Pho2	0.982	94.6	91.8	51.11

On comparing the values of the entropy of activation ΔS_a in (Table 5), it is clear that ΔS_a is more positive in presence of the studied inhibitor compared to free acid solution. The increase of ΔS_a in the presence of inhibitors implies that the activated Pho1 and Pho2 in the rate determining step represent an association rather than a dissociation step [32].

3.4. Adsorption isotherm and thermodynamic parameter

Adsorption isotherms are usually used to describe the adsorption process. The establishment of adsorption isotherms that describe the adsorption of a corrosion inhibitor can provide important clues to the nature of the metal-inhibitor interaction. Adsorption of the organic molecules occurs as the interaction energy between molecule and metal surface is higher than that between the H_2O molecule and the metal surface [33]. The best correlation between the experimental results and isotherm functions was obtained using the Langmuir adsorption isotherm intercepted by the following equation:

$$\frac{C}{\theta} = \frac{1}{K} + C \qquad (10)$$

Where C is the inhibitor concentration, K is the equilibrium constant and θ is the surface coverage. From the values of surface coverage, the linear regressions between C/θ and C are calculated by computer, and the parameters of adsorption are listed in Table 6. Figure 9 shows the relationship between C/θ and C at 308 K. these results indicate that the adsorption of inhibitor onto steel surface agrees the Langmuir adsorption isotherm.

The obtained values of ΔG^{o}_{ads} show a good correlation among thermodynamic parameters; those results ensure the spontaneity of the adsorption process and the stability of the adsorbed layer on the steel surface as well as strong interaction between the inhibitors and the metal surface [34].

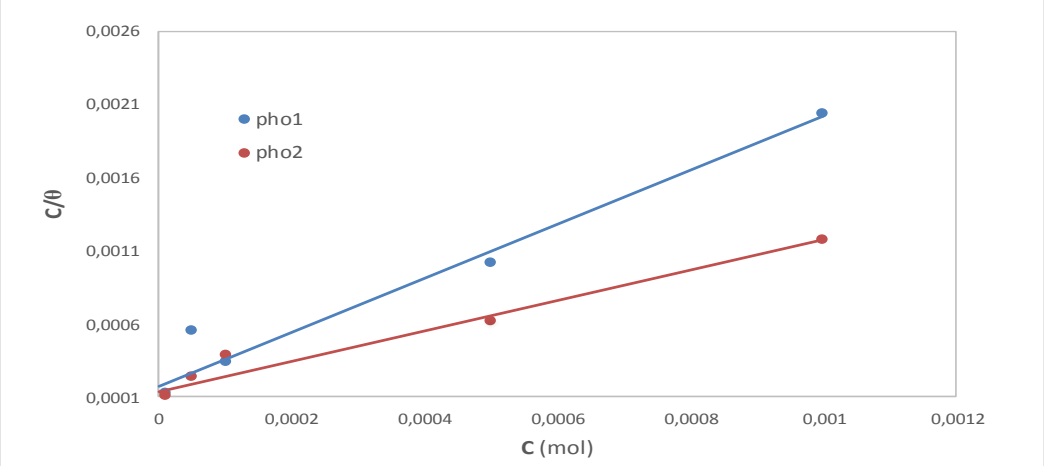

Figure 9: Langmuir adsorption isotherm of Pho1 and Pho2 on steel in 1M H_2SO_4 at 308 K.

Table 6: Adsorption parameters of the linear regression between C/θ and C of Pho1 and Pho2

Inhibitor	R^2	ΔG^{o}_{ads} (kJ/mol)
Pho1	0.9576	-32.08
Pho2	0.9537	-33.85

Table 6 shows the negative values of ΔG^{o}_{ads} indicate the spontaneity of adsorption of the inhibitor molecules on the mild steel surface [35]. In general, ΔG^{o}_{ads} values below -20 kJ mol^{-1} are due to the physisorption of the inhibitor, whereas ΔG^{o}_{ads} values above -40 kJ mol^{-1} are attributed to the chemisorption of the inhibitor molecules on metal surface. The values of ΔG^{o}_{ads} are -32.08 kJ mol^{-1} and -33.85 kJ mol^{-1} for Pho1 and Pho2, respectively. The calculated values of $|\Delta G^{o}_{ads}|$ of Pho in H_2SO_4 indicate that the adsorption mechanism of Pho1 and Pho2 on mild steel involves both chemisorption and physisorption [36-38]. Owing to the adsorbed water molecules on the surface of mild steel, it may be assumed that the adsorption occurs first due to the electrostatic interaction, and then the removal of water molecules from the surface is accompanied by chemical interaction between the metal surface and the adsorbate [39]. Moreover, the value of ΔG^{o}_{ads} for Pho2 is lower than that for Pho1, further demonstrating that Pho2 exhibits the stronger tendency to adsorb on metal surface.

4. Conclusions

Two phosphonate derivatives of Pho1 and Pho2 are good inhibitors for the corrosion of mild steel in 1M H_2SO_4 solution. η increases with the inhibitor concentration but decreases with temperature. Both Pho1 and Pho2 act as mixed-type inhibitors. EIS spectra exhibit a large capacitive loop at high frequencies followed by a small inductive loop at low frequency values. The presence of inhibitor in 1M H_2SO_4 solutions increases R_t while reduces C_{dl}. The value of apparent activation energy (E_a) in the presence of inhibitors are higher than that in the absence of inhibitor.

References

1. Poornima T., Jagannatha N., NityanandaShetty A., *Port. Electrochim. Acta* 28 (2010) 173.
2. Kumar P., Shetty A.N., *Surf. Eng. Appl. Electrochem*. 49 (2013) 253.
3. Prajila M., Sam J., Bincy J., Abraham J., *J. Mater. Environ. Sci.* 3 (2012) 1045.
4. Naik U.J., Panchal V.A., Patel A.S., Shah N.K., *J. Mater. Environ. Sci.* 3 (2012) 935.
5. Zarrouk A., Hammouti B., Zarrok H., Warad I., Bouachrine M., *Der Pharm. Chem*. 3 (2011) 263.
6. Ghazoui A., Bencaht N., Al-Deyab S.S., Zarrouk A. , Hammouti B., Ramdani M., Guenbour M. *Int. J. Electrochem. Sci*. 8 (2013) 2272.
7. Zarrouk A., Hammouti B., Zarrok H., Bouachrine M., Khaled K.F., Al-Deyab S.S. *Int. J. Electrochem. Sci*. 7 (2012) 89.
8. Ghazoui A., Saddik R., Benchat N., Guenbour M., Hammouti B., Al-Deyab S.S., Zarrouk A. *Int. J. Electrochem. Sci*.7 (2012) 7080.
9. Zarrouk, A., Hammouti, B., Dafali, A., Bentiss, F., *Ind. Eng. Chem. Res*. 52 (2013) 2560.
10. Zarrok H., Oudda H., El Midaoui A., Zarrouk A., Hammouti B., Ebn Touhami M., Attayibat A. , Radi S., Touzani R., *Res. Chem. Intermed*. 38 (2012) 2051.
11. Belayachi M., Serrar H., Zarrok H., El Assyry A., Zarrouk A., Oudda H., Boukhris S., Hammouti B., Ebenso Eno E., Geunbour A., *Int. J. Electrochem. Sci.,* 10 (2015) 3010.
12. Elaoufir Y., Bourazmi H., Serrar H., Zarrok H., Zarrouk A., Hammouti B., Guenbour A., Boukhriss S., Oudda H. *Der Pharm. Lett.* 6 (2014) 526.
13. Abdallah M., Atwa Sh. T., Abdallah N. M., El-Naggar I. M., Fouda A. S., *Anti. Corros. Method. M*. 58 (2011) 31.
14. Abdallah M., Asghar B. H., Zaafarany I., Sobhi M., *Metal. Phys. Chem. surf*. 49 (2013) 485.
15. Abdallah M., Zaafarany I., Khairou K. S., Sobhi M., *Int. J. Electrochem. Sci*. 7 (2012) 1564.
16. Hegazy M. A., *Corros. Sci*. 51 (2009) 2610.
17. Badawi A. M., Hegazy M. A., El-Sawy A. A., Ahmed H. M., Kamel W. M., *Mater. Chem. Phys*. 124 (2010) 458.
18. Yactine B., Ganachaud F., Senhaji O., Boutevin B. *Macromolecules*. 38 (2005) 2230.
19. Senhaji O., Robin J. J., Achchoubi M., Boutevin B. *Macromol. Chem. Phys*. 205 (2004) 1039.
20. Ferreira E. S., Giancomelli C., Giancomelli F. C., Spinelli A., *Mater. Chem. Phys*. 83 (2004) 129.
21. Riggs O. L., Nathan C. C., Houston, TX, *Jr. Corrosion Inhibitors*. (1973) 109.
22. Labjar N., Lebrini M., Bentiss F., Chihib N.E., El Hajjaji S., Jama C., *Mater. Chem. Phys.* 6 (2010) 119.
23. Lagreneé M., Mernari B., Bouanis M., Traisnel M., Bentiss F., *Corros. Sci*. 44 (2002) 573.
24. Singh A. K., Quraishi M. A., *Corros. Sci.* 52 (2010) 152.
25. Lebrini M., Lagreneé M., Vezin H., Traisnel M., Bentiss F., *Corros. Sci*. 49 (2007) 2254.
26. Gopi D., Govindaraju K. M., Kavitha L., *J. Appl. Electrochem*. 40 (2010) 1349.
27. Benali O., Larabi L., Traisnel M., Gengembre L., Harek Y., *Appl. Surf. Sci*. 253 (2007) 6130.
28. McCafferty E., and Hackerman N., *J. Electrochem. Soc*. 119 (1972) 146.
29. Muralidharan S., Phani K. L. N., Pitchumani S., Ravichhandran S., Iyer S. V. K., *J. Electrochem. Soc.* 142 (1995) 1478.
30 Popova A., Sokolova E., Raicheva S., Christov M., *Corros. Sci.* 45 (2003) 33.
31. Guan N. M., Xueming L., Fei L., *Mater. Chem. Phys*. 86 (2004) 59.
32. El-Awady A. A., Abd El-Naby B. A., Aziz S. G., Khalifa M., Al-Ghamdey H. A., *Int. J. Chem.*,1 (1990) 169.
33. Moretti G., Quartarone G., Tassan A., Zingales A., *Mater. Corros*. 45 (1994) 641.
34. Tang L., Li X., Li L., Qu Q., Mu G., Liu G., *Mater. Chem. Phys*. 94 (2005) 353.
35. Abdallach M., *Corros. Sci*. 44 (2002) 717.
36/ Yurt A., Bereket G., Kivrak A., Balaban A., Erk B., *J. Appl. Electrochem*. 35 (2005) 1025.
37. Fekry A. M., Mohamed R. R., *Electrochim. Acta*. 55 (2010) 1933.
38. Saliyan V. R., Adhikari A. V., *Corros. Sci*. 50 (2008) 55.
39. Vračar L. M., Dražic D.M., *Corros. Sci*. 44 (2002) 1669.